NORSAR

NORSAR Scientific Report No. 2-1999/2000

Semiannual Technical Summary

1 October 1999 - 31 March 2000

Frode Ringdal (ed.)

Kjeller, May 2000

6.4 Recent profiling experiments in the Spitsbergen area - calibration data for the SPITS array

Introduction

In 1992, the seismic array SPITS was installed on Spitsbergen, the main island of the Svalbard Archipelago. Today, this array is part of the International Monitoring System (IMS) network as one of its auxiliary seismic stations. The Svalbard Archipelago is located at one edge of the Eurasian plate, with the continental shelf and the boundary with the North American plate 100 to 500 km to the west and the north. This plate boundary is part of the mid-Atlantic ridge system (MARS) and is characterized by its high natural seismicity. To the east and to the south of Svalbard is the large continental shelf which forms the Barents Sea. The last Soviet nuclear test took place on Novaya Zemlya, an island group also located in the Barents Sea and only about 1100 km apart from the SPITS array.

The seismic travel times for local and regional events around the SPITS array are influenced by the large variations in the crustal structure around Svalbard. During the last years several scientific and commercial reflection and refraction experiments have been undertaken in the sea around the Svalbard Archipelago. Airgun shots and small explosions conducted for these experiments were observed with the SPITS array.

Høgden (1999) interpreted SPITS data from a commercial reflection survey in the Barents Sea east of the Svalbard Archipelago. This survey was carried out by the Norwegian Petroleum Directorate (NPD) from August 24 to October 4, 1994 using airgun sources along 14 profiles. He analyzed two of these profiles in more detail and interpreted the first P onsets from sources at distances between 170 and 350 km from SPITS. The cross-over distance of Pn could be observed at about 210 km which corresponds to a depth of the Mohorovicic discontinuity of about 37 km. However, one disadvantage of these data was the short time difference between the single airgun shots of 10 seconds only, so that the coda of the first onset and later arrivals interfered with the signal of the next shot.

Scientific reflection and/or refraction surveys usually do not have this problem because in such experiments the reflections/refractions from structures in deeper parts of the crust and the uppermost mantle are also of interest. Therefore larger time differences are used between the consecutive shots.

Recently, exact source parameters from such experiments became available and resulted in a unique set of ground-truth information that can be used to calibrate local and regional travel-time curves around SPITS. The topic of this contribution is to document the data of four seismic surveys conducted in 1997 and 1999, as a first step towards a systematic investigation of all available seismic survey informations around the Svalbard Archipelago.

Data from seismic profiling west and north-west of Spitsbergen

During the arctic summers of 1997 and 1999 the German Institute for Polar and Oceanic Sciences (Alfred-Wegener-Institute) carried out in cooperation with the Polish Academy of Sciences four reflection/refraction experiments to investigate the structure of the continental shelf, the slope of the shelf, the deep-see area, and the corresponding part of the mid-atlantic ridge system west and north-west of Spitsbergen. Along these four profiles airgun shots were carried

out every one minute during which the vessel moved about 180 meters. In addition, on three of the profiles, small explosions were also fired using 25 or 50 kg of conventional explosives. The not yet published source information (for more details see Table 6.4.1) for these experiments was kindly supplied to us by Oliver Ritzmann of the Alfred-Wegener-Institute (pers. communication). Shots along all profiles were observed at SPITS with reasonably high SNR. The airgun shot profiles and the positions of the 50 explosions on the three profiles of 1999 are plotted on maps in Fig. 6.4.1.

Because all exact airgun positions are available, the data could be analyzed using the double-beam technique (Krüger *et al.*, 1993) to improve the signal-to-noise ratio (SNR). The single airgun shots were generally detectable at the single sites of the SPITS array. Using the classical beamforming, we can theoretically improve the SNR by a factor of 3 because SPITS consists of 9 vertical sensors (receiver beam). The horizontal distance between the single airgun shots was about 180 meters and about 5 airgun shots cover a distance which is about the aperture of the SPITS array (1 km). So, without larger loss of coherence of the signals, we can also sum up the energy of several airgun shots to one seismogram (source beam). Combining both beam types, we get the so called double beam with a theoretically SNR increase of up to a factor of 6.7 with respect to a single station observation, if we can add 9 sites and 5 airgun shots. In Fig. 6.4.2 the advantage of this procedure is shown for a short part of a seismogram section with data from Profile 1. At the bottom, the single seismograms as observed at a single site of the SPITS array (SPB4) are shown, in the middle we see the corresponding receiver beams of the SPITS array, using the theoretical backazimuth and a common apparent velocity of 9 km/s in the beamforming. At the top, the result of the double beam technique is shown: we stacked up to 5 single-airgun-shot beams to one double beam. The stepwise improvement of the SNR is obvious.

In Fig. 6.4.3 the entire seismogram section of the double beams for Profile 1 is shown. For distances below about 0.9 deg from the array, a lower crust phase is clearly seen as the first onset. The second onset is the Moho reflection PmP. Around the cross-over distance of Pn the picture becomes very complicated: the onsets are delayed and the travel-time curve of the first onsets is complex. This is the region where the seismic waves bottom below the west coast of Spitsbergen, a region with crustal thickening and a known north-south striking tectonic boundary (see *e.g.* Eiken, 1994). At distances larger than about 1.8 deg the observed amplitudes decrease drastically, which could be a damping effect due to the vicinity of the MARS.

Fig. 6.4.4 shows the double beams calculated for the observations of Profile 2. As seen on the map (Fig. 6.4.1, upper part) the ship was moving for a large part of the profile at approximately the same distance from SPITS (1.8 to 2 deg). This explains the higher density of observations in this distance range in the seismogram section. The quality of the Pn onsets differ along the profile and for larger distances close to the MARS (>~ 3 deg) onsets from the airgun shots are hardly identifiable. At distances between 1.8 and 2.3 deg, secondary P onsets with larger amplitudes than the first onstes are visible. This feature can also be seen on the seismogram section for the explosion sources along the same profile (Fig. 6.4.1, bottom). The distance between the single explosion was too large to apply the double-beam technique, therefore Fig. 6.4.5 contains only the corresponding receiver beams. The theoretical travel-times calculated for a surface focus with the spherical standard Earth model AK135 (Kennett *et al.*, 1995) are shown. The P velocities of this model are shown in Fig. 6.4.9, and the travel-time curves for the distance range covered by the profiles investigated here can be seen in Fig. 6.4.10.

Profile 3 (Fig. 6.4.6) approximately covers the same distance range as Profile 2. But on this profile the secondary P onsets are much more pronounced. The corresponding seismogram section of the explosion sources (Fig. 6.4.7) shows clear variations in the first P onset times indicated by black bars. The array beams and the onset times picked (bars) were also added to the seismogram section in Fig. 6.4.6. Note that the observations of the explosion sources with their higher SNR help to identify onsets of the airgun shots. Fig. 6.4.7 also contains travel-time curves calculated for a regional velocity model of the Barents Sea (Kremenetskaya and Asming, 1999) which cannot be used to explain these observations. The velocities of this model were also plotted in Fig. 6.4.9, and Fig. 6.4.10 also contains the travel-time curves for the Barents Sea model for the distance range covered by the profiles investigated here.

Finally, Fig. 6.4.8 shows the double beams of the Profile 4 observations. This profile was located between Profiles 1 and 2. Again, we can identify different P onsets at distances up to 1.8 deg. For larger distances (> ~ 2.6 deg) the airgun shots were carried out on the other side of the MARS (see also Fig. 6.4.1, top) and no seismic energy of these distant airgun shots can be identified in the seismogram section.

Conclusions

- The structure of the crust and the uppermost mantle around the IMS station SPITS is very heterogeneous.
- Observed travel times from GT0 events show strong deviations from predictions by standard models.
- Airgun shots of deep seismic profiling experiments (DSS) can be observed with small aperture arrays up to several hundred kilometers away. Therefore, source parameters of commercial and scientific DSS experiments represent useful ground-truth information.
- Numerous DSS experiments in the sea around Spitsbergen enabled us to derive azimuth-dependent travel-time curves for local and regional distances.
- The ground-truth data base will be used to reanalyze in more detail the previously reported large slowness deviations observed at SPITS (*e.g.* Kværna *et al.*).
- Exact travel times for distances up to of about 350 km are now available for different azimuth directions from the SPITS array. This travel time information will be used for a more precise location of local and regional events observed at SPITS.

J. Schweitzer

References

Eiken, O., editor (1994): Seismic atlas of western Svalbard - a selection of regional seismic transects. Norsk Polarinstitutt Oslo, *Meddelelser **130***, 73 pp. and 14 enclosures.

Høgden, S. (1999): Seismotectonics and crustal structure of the Svalbard region. Cand. Scient. thesis, Department of Geology, University of Oslo, 142 pp.

Kennett, B.L.N., Engdahl, E.R., and Buland, R. (1995): Constraints on seismic velocities in the Earth from traveltimes, *Geophys. J. Int. **122***, 108-124.

Kremenetskaya, E. and V. Asming (1999): Location calibration of the Barents region. In: Workshop on IMS location calibration, IDC technical experts group on seismic event location, Oslo, 12 - 14 January 1999, Technical Documentation.

Krüger, F., M. Weber, F. Scherbaum and J. Schlittenhardt (1993): Double beam analysis in the core-mantle boundary region. *Geophys. Res. Lett. **20***, 8089-8115.

Kværna, T., J. Schweitzer, L. Taylor, and F. Ringdal (1999): Monitoring the European Arctic using regional generalized beamforming. *Semiannual Technical Report 1 October 1998 - 31 March 1999. NORSAR Sci. Report **2-98/99***, Keller, Norway, 78-94.

Table 6.4.1. Parameters of the profiles investigated. Date gives the days on which this profile was carried out, Lat-1 (Lat-2) and Lon-1 (Lon-2) are the start (end) points of the profiles, and Source indicates the source type (A for airguns, E for conventional explosions) and the number of sources on this profile.

Profile	Date	Lat-1 [deg]	Lon-1 [deg]	Lat-2 [deg]	Lon-2 [deg]	Source
1	06 September 1997 - 07 September 1997	77.82908	16.66815	76.77796	6.83346	A (1597)
2	21 August 1999 - 23 August 1999	78.82621	0.24860	80.18131	17.20085	A (2476)
2	21 August 1999 - 22 August 1999	79.74350	10.0110	79.21780	4.13780	E (25)
3	26 August 1999 - 27 August 1999	80.96566	7.09669	78.82445	11.27687	A (1455)
3	26 August 1999	79.80120	10.25390	80.70650	8.56010	E (20)
4	01 September 1999 - 02 September 1999	78.94233	12.01583	78.50227	0.03603	A (1628)
4	03 September 1999	78.91730	9.56190	78.87150	8.54527	E (5)

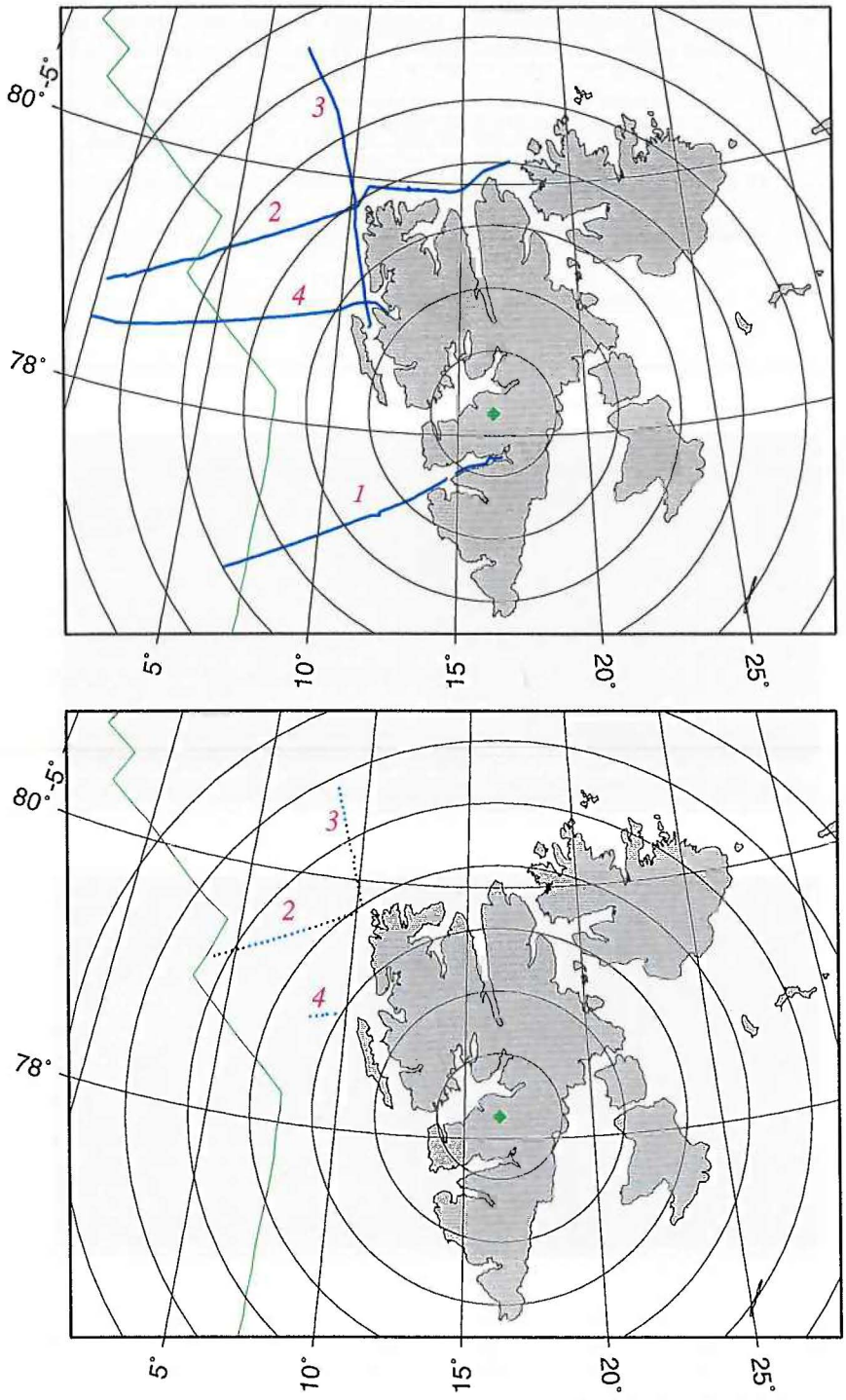

Fig. 6.4.1. *Maps of the Spitsbergen area showing the location of the SPITS array, equidistant circles around the array in steps of 0.5 deg, and the plate boundary (MARS) between the Eurasian and the North American plate. The upper map shows the positions of the four airgun profiles and the lower map the positions of the three profiles shot with conventional explosives (for more details see Table 6.4.1).*

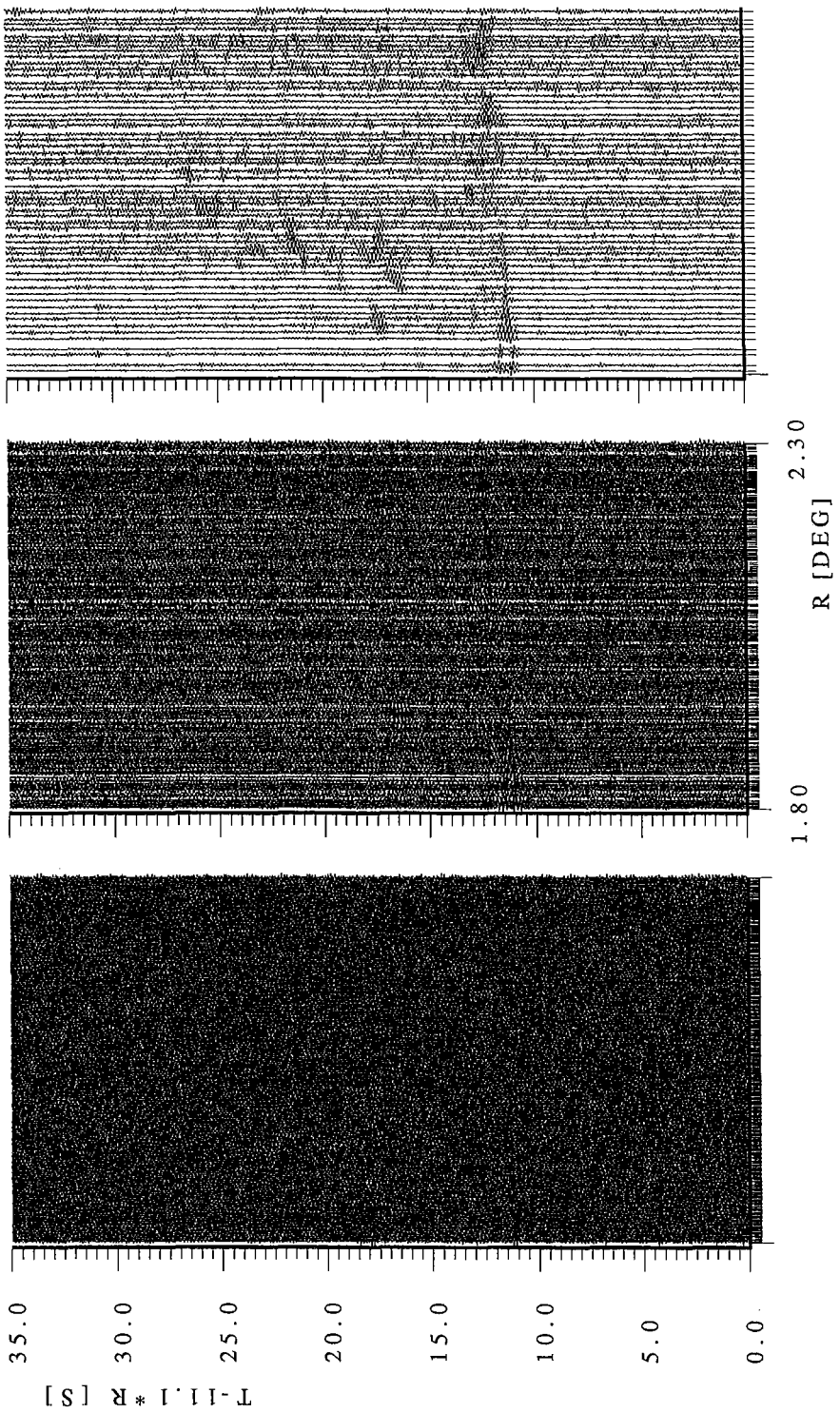

Fig. 6.4.2. *This figure shows the improvement of the SNR due to the double-beam technique (Krüger et al., 1993). At the bottom, single seismograms of station SPB4 from airgun shots of Profile 1 are shown. The epicentral distance is between 1.8 and 2.3 deg, the seismograms are filtered with a Butterworth bandpass filter between 5 and 10 Hz, and the traces were individually normalized. In the middle part of the figure the corresponding beams of the SPITS array are shown, and at the top the double beams after summing up to 5 single-airgun-shot beams to a common beam.*

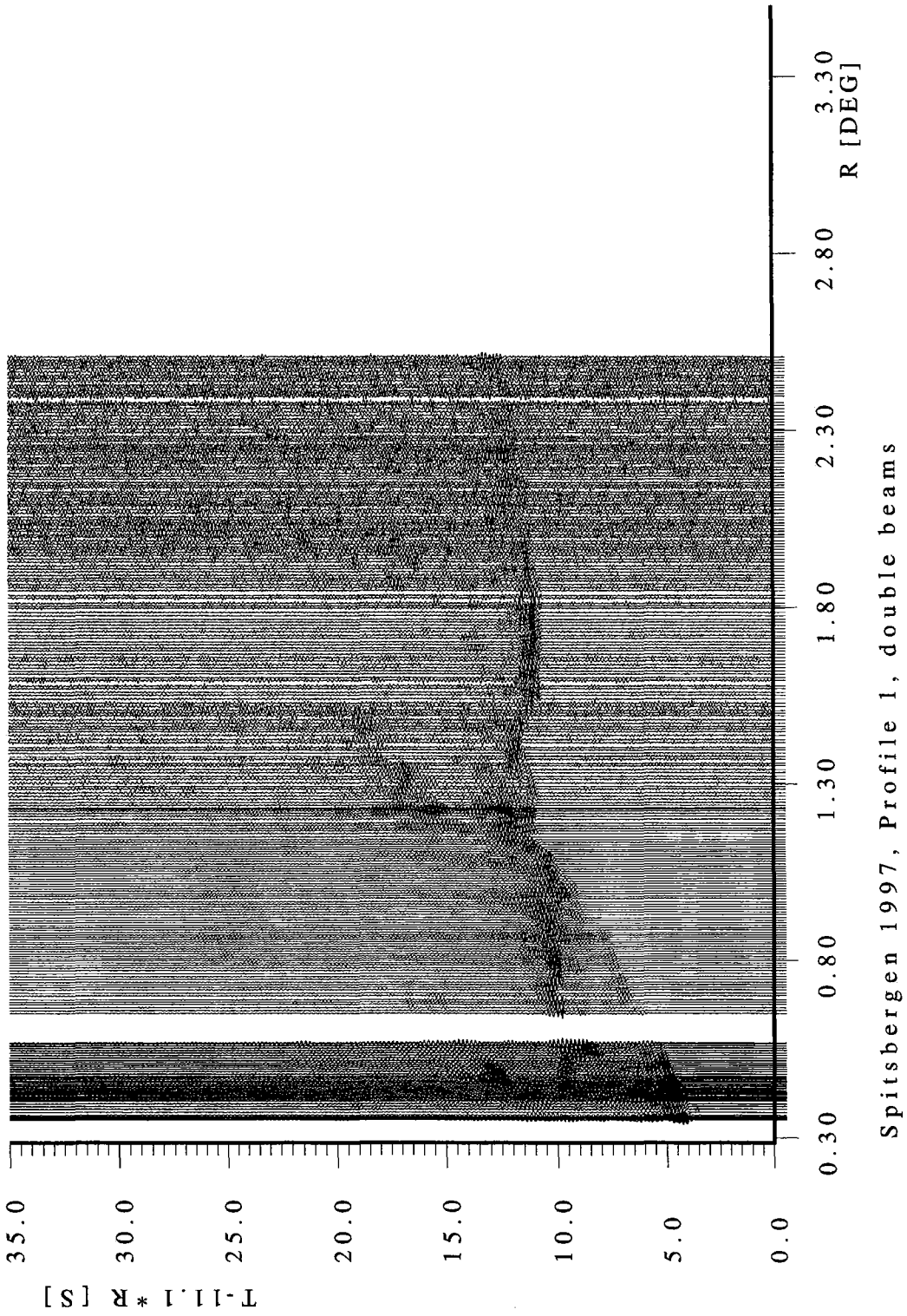

Fig. 6.4.3. *Seismogram section of double beams calculated from Profile 1 shots observed at SPITS. As in Fig. 6.4.2, all seismograms are filtered between 5 and 10 Hz and all traces were individually normalized. The seismogram section was reduced with 11.1 s/deg which corresponds to an apparent velocity of 10 km/s. The larger gap in the seismogram section is due to an island which the ship had to circumnavigate (gap in the blue line for Profile 1 in Fig. 6.4.1).*

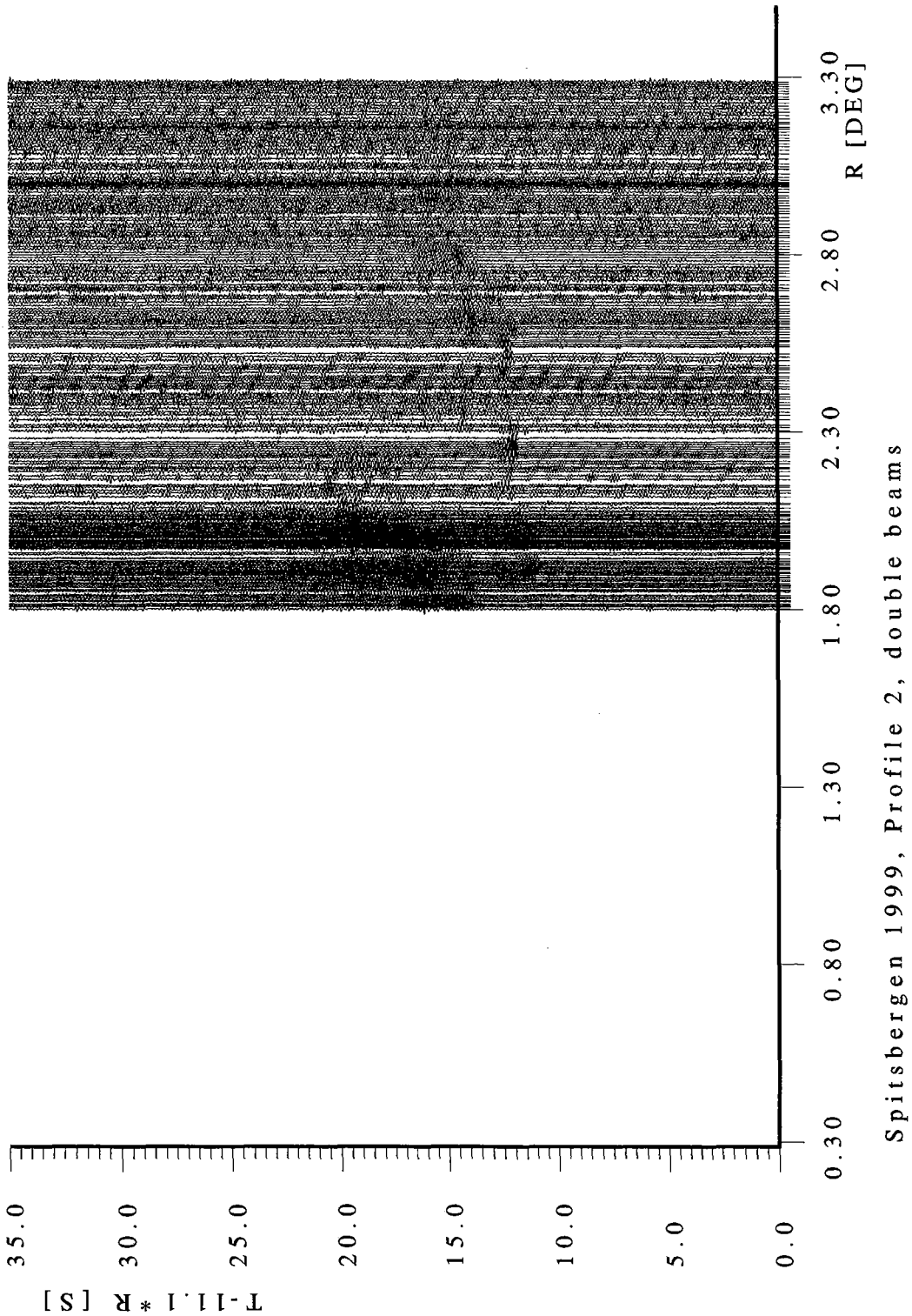

Fig. 6.4.4. *Seismogram section of double beams calculated from Profile 2 airgun shots observed at SPITS. Filters and reduction velocity are as used for Fig. 6.4.3.*

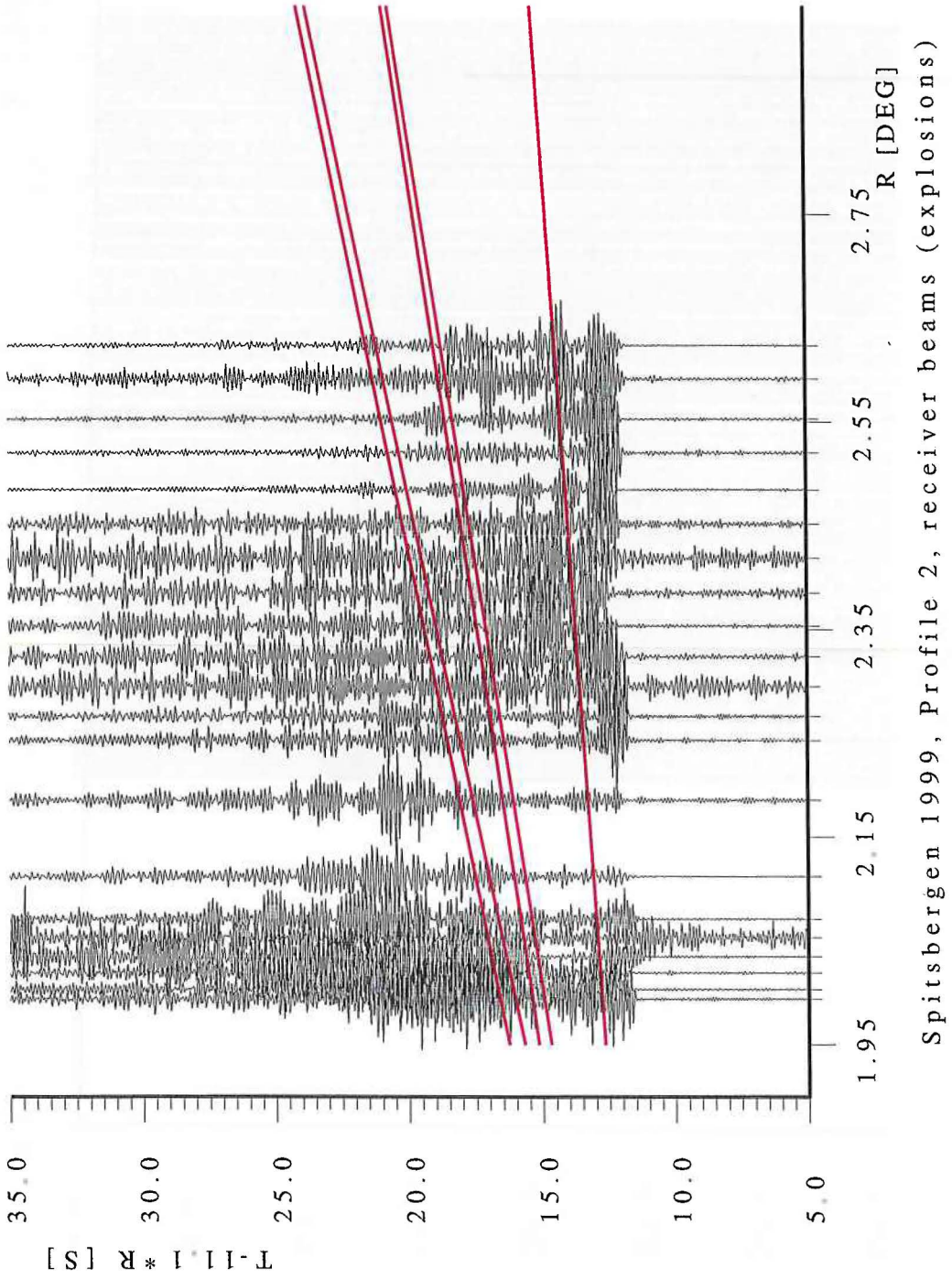

Fig. 6.4.5. *Seismogram section as in Fig. 6.4.4, but now for receiver beams for the observed conventional explosions along Profile 2 (see Fig. 6.4.1, bottom). In addition, theoretical travel-time curves for a surface source calculated using the spherical Earth model AK135 (Kennett et al., 1995) are plotted.*

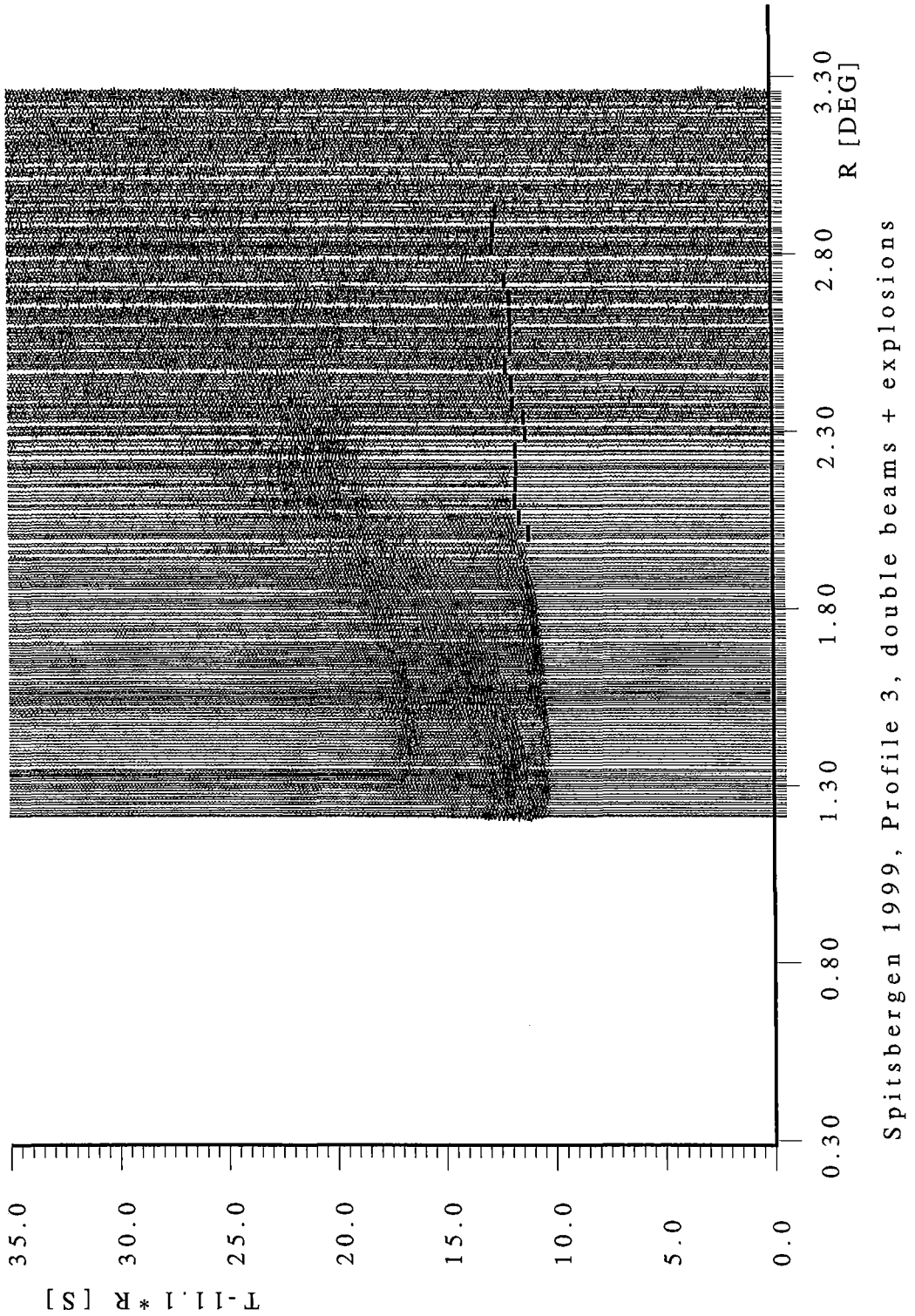

Fig. 6.4.6. *Seismogram section of double beams as in Fig. 6.4.3, but for the Profile 3 observations. In addition, the receiver beams of the observed explosions along this profile as shown in the expanded plot of Fig. 6.4.7 are included in this plot. The vertical bars indicate the first onset times from Fig. 6.4.7.*

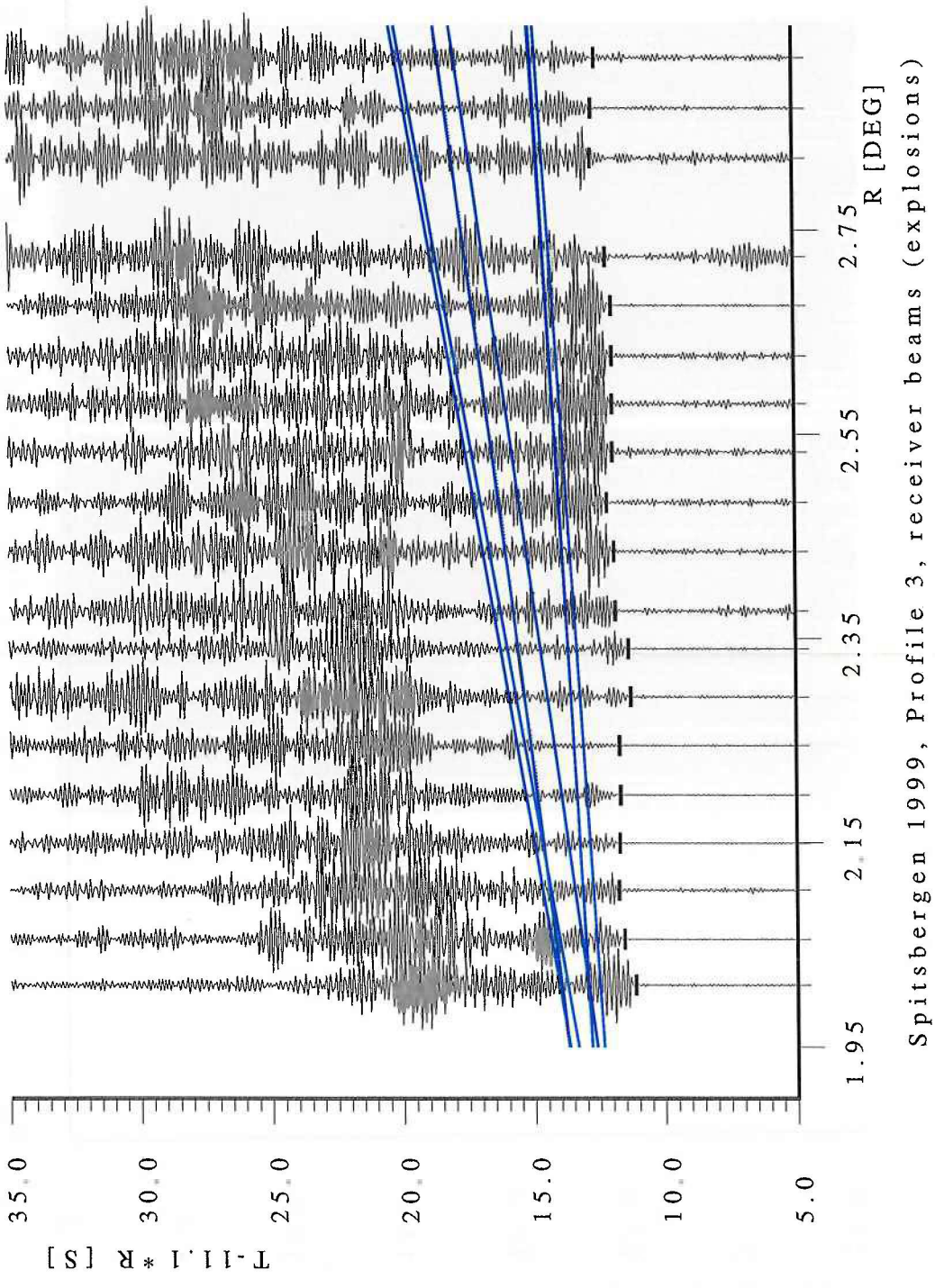

Fig. 6.4.7. *Seismogram section for the receiver beams for the observed conventional explosions conducted along Profile 3 (see also Fig. 6.4.1, bottom). In addition, theoretical travel-time curves for a surface source calculated using a regional model for the Barents region (Kremenetskaya and Asming, 1999) are plotted. The vertical bars are the first onset times as picked in this study.*

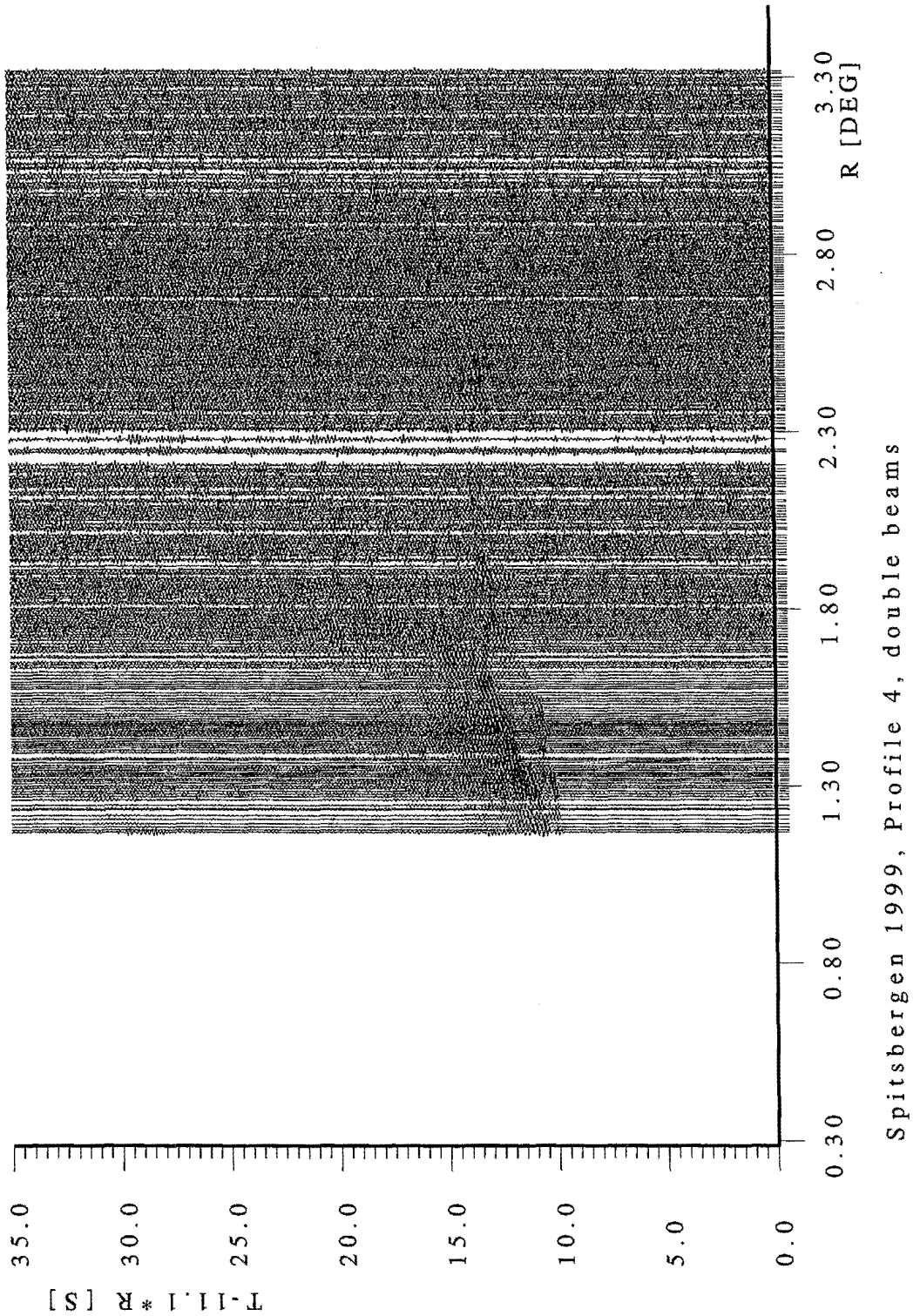

Fig. 6.4.8. *Seismogram section of double beams as in Fig. 6.4.3, but for the Profile 4 observations.*

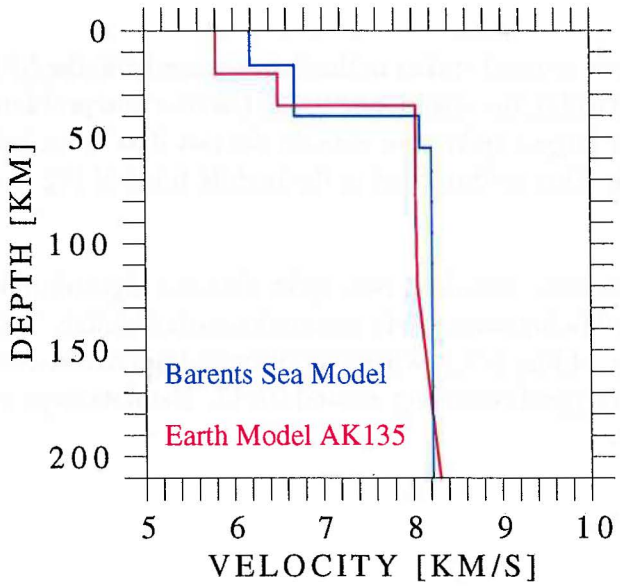

Fig. 6.4.9. *The two P-velocity models used as reference in this study. The model AK135 is a global Earth model (Kennett et al., 1995) and the Barents Sea model is a regional velocity model (Kremenetskaya and Asming, 1999).*

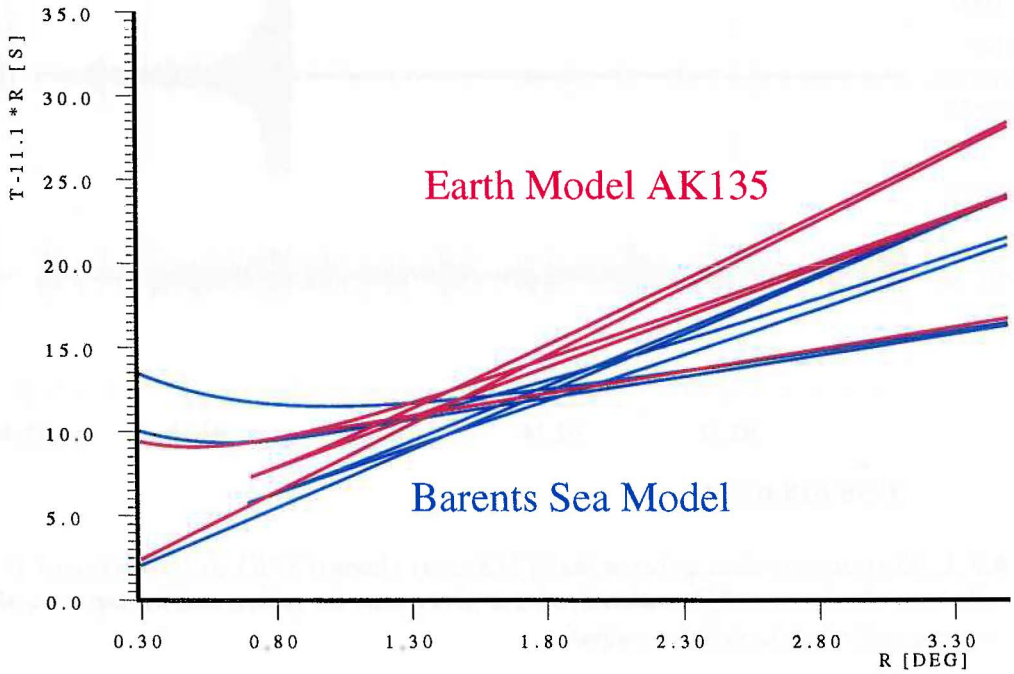

Fig. 6.4.10. *P phase travel-time curves for the two models used as reference in this study (see Fig. 6.4.9).*